TRANSNAV
http://www.transnav.eu
the International Journal
on Marine Navigation
and Safety of Sea Transportation
Volume 14
Number 2
June 2020

DOI: 10.12716/1001.14.02.14

Waypoint Path Controller for Ships

M. Tomera & Ł. Alfuth
Gdynia Maritime University, Gdynia, Poland

ABSTRACT: The paper presents and discusses tests of a waypoint controller used to sail a ship along the desired route. The planned desired route for the moving ship is given as a set of waypoints connected with straight lines. The ship's control is based on the rudder blade deflection angle as a commanded parameter. The task of the controller is to determine the rudder angle which will allow the ship to sail along the desired route segment. The controller algorithm consists of two parts, the first of which is used for controlling the ship motion along linear segments of the desired route, while the second part is used when changing to the next route segment. A switching mechanism is designed to choose the relevant part of the control algorithm. The quality of operation of the ship motion control algorithm was tested on the training ship *Blue Lady*, at the Ship Handling Research and Training Centre located on the lake Silm at Kamionka near Iława, Poland.

1 INTRODUCTION

The desired route of a given ship is usually expressed using waypoints (Fossen, 2011). This description method is extremely attractive, since the route can be easily stored in the onboard computer's memory. Waypoints can be designated and programmed before or during the cruise, taking into account such factors as weather conditions, avoiding obstacles, and mission planning (Śmierzchalski & Łebkowski, 2002; Lazarowska, 2016; Lisowski, 2016). Each waypoint, defined in Cartesian coordinates (x_i, y_i), is used for creating the desired route as a set of straight line segments connecting pairs of successive waypoints. When the ship reaches the designated acceptance circle surrounding the waypoint i, the path is switched to the next line segment connecting waypoints i and i+1. In a more advanced solution, arcs of circles connecting line segments of the route are defined around each waypoint, and are then used to determine the desired turning at this point (Kula & Tomera, 2017). Once the waypoints are established, it is usually desirable for the sea unit to track the waypoints as closely as possible, even in the presence of unknown environmental disturbances.

Analyzing the operation of ship control systems for surface ships moving along the desired route began in the 1980s. In principle, it is easy to design a system to control the ship course along the set trajectory passed from a conventional autopilot by using the information obtained from the positioning system (Amerongen & Nauta Lemke, 1986). However, better quality is obtained when considering the system as a whole, including the ship, the ship-acting environment, and the regulator, as in this case all relevant state variables can be used in control synthesis. The entire system can be analyzed through the use of techniques known as analytical control strategies, such as self-tuning control (Kallstrom, 1982), *LQG* (Holzhutter, 1990; Bertin, 1998; Morawski & Pomirski, 1998), adaptive control (Chocianowicz &

Pejaś, 1992), H_∞ (Messer & Grimble, 1993) and *LMI* (Miller & Rybczak, 2015).

A common feature of all the above analytical control strategies is their dependence on the reliability of the mathematical model describing the maneuvering dynamics of the ship. In addition, it is often necessary to linearize the ship's model before applying the above analytical control strategies.

In order to avoid the above difficulties associated with the accuracy of the applied mathematical model of ship dynamics, other control strategies, making use of the fuzzy set theory (Vukic et al., 1998; Velagic et al., 2003; Gierusz et al., 2007; Ahmed & Hasegawa, 2016; Yu & Xiang, 2017), artificial neural networks (Zhang et al., 1996; Kula, 2015; Zhuo & Guo) and nonlinear control (Pettersen & Lefeber, 2001; Do & Pan, 2003; Fredriksen & Pettersen, 2006; Baker et al. 2013; Witkowska & Śmierzchalski, 2018) have also been developed.

Conventional ships are usually equipped with one or two main propellers for controlling the surge velocity and fins for controlling the course. Even if additional transverse thrusters are installed, they do not provide a significant extra force at transit speeds. This means that independent control is possible with only two degrees of freedom (DOF): surge and yaw. In this article, the problem of control is defined in such a way that the ship follows straight line segments between the route waypoints at constant speed, and the ship motion control is performed using the rudder blade as a commanded parameter.

2 PROBLEM FORMULATION

The movement of a ship sailing on the water surface is described in three degrees of freedom. Two coordinate systems are used for its description (Figure 1). The first of them is the Earth-fixed coordinate system (X_N, Y_N), related to the water map, in which the X_N-axis points north and the Y_N-axis points east. The other coordinate system (X_B, Y_B) is associated with a moving ship, and its origin is on the waterline, at the point consistent with the position of the center of gravity of the ship. The state variables $\boldsymbol{x}$ describing the ship movement are collected in two vectors $\boldsymbol{\eta} = [x, y, \psi]^T$ and $\boldsymbol{\nu} = [u, v, r]^T$ (Fossen, 2011).

The components of the vector $\boldsymbol{\eta}$ are defined in the Earth-fixed coordinate system (X_N, Y_N), while those of the vector $\boldsymbol{\nu}$ in the body-fixed coordinate system (X_B, Y_B). The resultant vector of the ship's movement status has the form

$$\boldsymbol{x} = [\boldsymbol{\eta}^T \ \boldsymbol{\nu}^T]^T = [x, y, \psi, u, v, r]^T \tag{1}$$

The velocity vector $\dot{\boldsymbol{\eta}}$ defined in the Earth-fixed coordinate system is associated with the velocity vector $\boldsymbol{\nu}$ determined in the body-fixed coordinate system using the following kinematic relationship

$$\dot{\boldsymbol{\eta}} = \boldsymbol{R}(\psi)\boldsymbol{\nu} \tag{2}$$

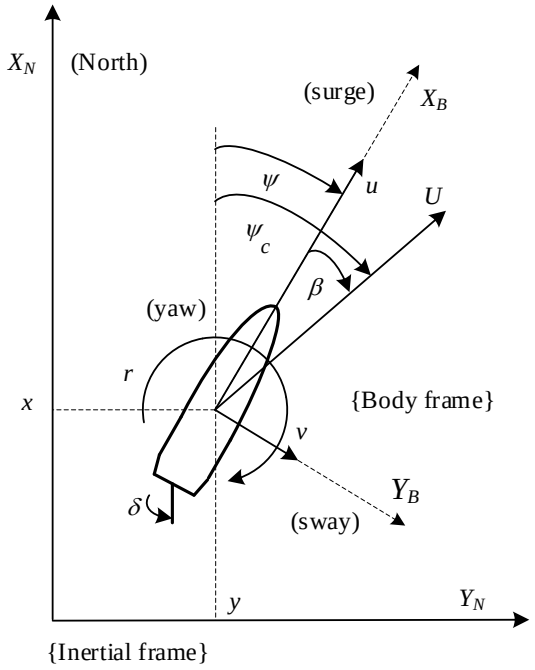

Figure 1. Quantities describing ship's movement in the horizontal plane, (X_N, Y_N) – Earth-fixed reference system, (X_B, Y_B) – body-fixed reference system, (x, y) – position coordinates, ψ – ship's course, u – surge speed, v – sway speed, r – yaw rate, U – total speed, δ – rudder angle, β - sideslip angle.

where $\boldsymbol{R}(\psi)$ is the rotation matrix determined from the formula

$$\boldsymbol{R}(\psi) = \begin{bmatrix} \cos\psi & -\sin\psi & 0 \\ \sin\psi & \cos\psi & 0 \\ 0 & 0 & 1 \end{bmatrix} \tag{3}$$

The ideal desired route of the ship consists of a number of linear segments N (Figure 2). The ship is assumed to move along straight line segments between the waypoints. The desired speed u_{dk} is assumed constant over each individual route segment. The course ψ_k resulting from the current route segment is the right-handed angle, relative to the X_N axis

$$\psi_k = \text{atan2}(y_{k+1} - y_k, x_{k+1} - x_k) \tag{4}$$

During the turning maneuver at a waypoint, the ship moves along a circular arc connecting the adjoining linear segments at this point. In order to be able to perform such a maneuver, it is necessary to start the turning maneuver at a distance L_k ahead of the waypoint, the length of which depends on the course difference between two consecutive linear route segments

$$L_k = f(\Delta\psi_k) = f(\psi_{k+1} - \psi_k) \tag{5}$$

and can be determined experimentally.

To facilitate determining the deviation of ship's position in relation to the implemented segment of

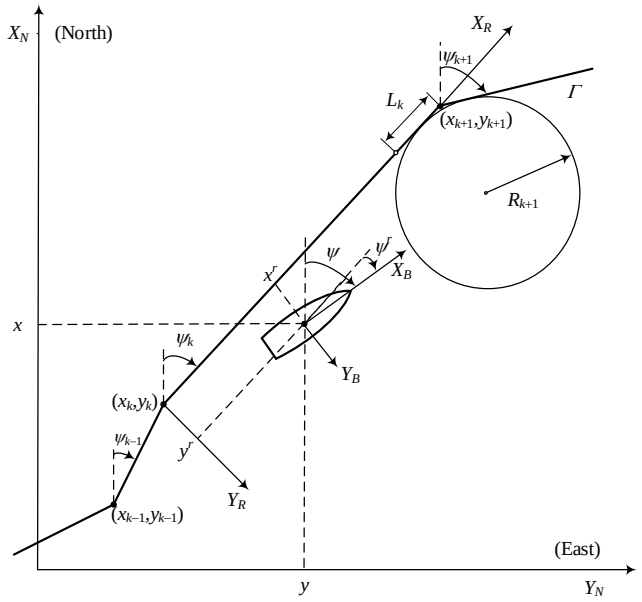

Figure 2. Concept of surface ship track-keeping along desired route

the desired route, the third coordinate system (X_R, Y_R) is introduced. The origin of this system is at the starting point of the executed line segment of the desired route (x_k, y_k), while the X_R-axis points towards the waypoint (x_{k+1}, y_{k+1}).

The control task consists in finding such an algorithm that will allow the ship to follow the ideal route of the passage (Figure 2). The control signal is assumed to be a two-element vector having the form

$$\boldsymbol{S}_c(t) = [\delta_c(t) \quad n_{gc}(t)]^{\mathrm{T}} \tag{6}$$

where $\delta_c(t)$ it is the commanded rudder blade deflection angle, whereas $n_{gc}(t)$ is the commanded rotational speed of the propeller.

3 MATHEMATICAL MODEL OF SHIP'S DYNAMICS AND ACTUATORS

The control plant is a 1:24 scale physical model of the tanker *Blue Lady*. The most important parameters of this model are summarized in Table 1.

Table 1. Main particulars of the training ship *Blue Lady*

Parameter	Value
Total length	L_{OA} = 13.78 (m)
Breadth	B = 2.38 (m)
Draft (full load)	T_d = 0.86 (m)
Displacement (full load)	Δ = 22.83 (m^3)
Position of center of gravity	x_G = 0.00 (m)

A complex mathematical model for this tanker was developed by Gierusz (2001). The model includes all actuators installed on the ship and allows to analyze its movement in the entire speed range.

In a general form, the mathematical model of ship's dynamics is given as

$$\boldsymbol{M}\dot{\boldsymbol{v}} + \boldsymbol{C}(\boldsymbol{v})\boldsymbol{v} + \boldsymbol{D}(\boldsymbol{v})\boldsymbol{v} = \boldsymbol{\tau} \tag{7}$$

The matrix $\boldsymbol{M}$ contains the parameters of inertia of the rigid body, its dimensions, weight, mass distribution, and volume, as well as the added weight coefficients

$$\boldsymbol{M} = \begin{bmatrix} m - X_{\dot{u}} & 0 & 0 \\ 0 & m - Y_{\dot{v}} & mx_G - Y_{\dot{r}} \\ 0 & mx_G - N_{\dot{v}} & I_z - N_{\dot{r}} \end{bmatrix} \tag{8}$$

The centripetal and Coriolis force matrix $\boldsymbol{C}$ contains hydrodynamic coefficients associated with the liquid in which the ship moves

$$\boldsymbol{C}(\boldsymbol{v}) = \begin{bmatrix} 0 & 0 & -m(x_G r + v) \\ 0 & 0 & (m - X_{\dot{u}})u \\ m(x_G r + v) & -(m - X_{\dot{u}})u & 0 \end{bmatrix} \tag{9}$$

The damping matrix $\boldsymbol{D}$ is associated with hydrodynamic damping forces and makes it possible to determine these forces for high velocities.

$$\boldsymbol{D}(\boldsymbol{v}) = \begin{bmatrix} -d_{11}(\boldsymbol{v}) & 0 & 0 \\ 0 & -d_{22}(\boldsymbol{v}) & -d_{23}(\boldsymbol{v}) \\ 0 & -d_{32}(\boldsymbol{v}) & -d_{33}(\boldsymbol{v}) \end{bmatrix} \tag{10}$$

where

$$d_{11}(\boldsymbol{v}) = X_{|u|u}\,|u|,$$
$$d_{22}(\boldsymbol{v}) = Y_{|u|v}\,|u| + Y_{|v|v}\,|v| + Y_{|r|v}\,|r|,$$
$$d_{23}(\boldsymbol{v}) = Y_{|u|r}\,|u| + Y_{|v|r}\,|v| + Y_{|r|r}\,|r|,$$
$$d_{32}(\boldsymbol{v}) = N_{|u|v}\,|u| + N_{|v|v}\,|v| + N_{|r|v}\,|r|,$$
$$d_{33}(\boldsymbol{v}) = N_{|u|r}\,|u| + N_{|v|r}\,|v| + N_{|r|r}\,|r|.$$

Table 2 presents all parameters related to the mathematical model of *Blue Lady* dynamics given by Eq. 7. The vector of forces acting on the ship's hull is composed of forces generated by the propeller and rudder blade and those generated by interacting external environmental disturbances.

$$\boldsymbol{\tau} = \left[\tau_X, \tau_Y, \tau_N\right]^{\mathrm{T}} = \boldsymbol{\tau}_{th} + \boldsymbol{\tau}_w \tag{11}$$

Table 2. Parameters of *Blue Lady* dynamics

No	Variable	Value	No	Variable	Value
1	m	22 934.4	11	$Y_{\|r\|v}$	–29 634.8
2	I_z	436 830.2	12	$Y_{\|u\|r}$	7 841.9
3	$X_{\dot{u}}$	–730.5	13	$Y_{\|v\|r}$	18 521.8
4	$Y_{\dot{v}}$	–18 961.8	14	$Y_{\|r\|r}$	12 502.0
5	$Y_{\dot{r}}$	0.0	15	$N_{\|u\|v}$	–9 984.6
6	$N_{\dot{v}}$	0.0	16	$N_{\|v\|v}$	–9 260.9
7	$N_{\dot{r}}$	–183 519.1	17	$N_{\|r\|v}$	–40 007.0
8	$X_{\|u\|u}$	–193.9	18	$N_{\|u\|r}$	–55 614.0
9	$Y_{\|u\|v}$	–2 350.9	19	$N_{\|v\|r}$	–12 502.0
10	$Y_{\|v\|v}$	–6 859.9	20	$N_{\|r\|r}$	–843 900.0

3.1 *Mathematical model of propeller and rudder blade*

For a propeller with a fixed blade angle, the generated thrust force is more or less proportional to the square of the shaft speed n_g. The propeller/rudder model can

be divided into two parts. The first part describes the nominal pressure (at rudder angle $\delta = 0$).

$$T = \begin{cases} k_{Tp} n_g^2 & n_g \geq 0 \\ k_{Tn} |n_g| n_g & n_g \leq 0 \end{cases} \tag{12}$$

The second part concerns additional forces: drag and lift, produced by the rudder blade associated with the propeller.

$$D = \begin{cases} 0.5 F_R \sin\delta, & n_g \geq 0 \\ 0 & n_g < 0 \end{cases} \tag{13}$$

$$L = \begin{cases} F_R \cos\delta, & n_g \geq 0 \\ 0 & n_g < 0 \end{cases} \tag{14}$$

where F_R is the operating force of the rudder blade, expressed as:

$$F_R = \begin{cases} k_{Fp} \cdot u_\delta^2 \sin(\delta + \beta_R) & u \geq 0 \\ k_{Fn} \cdot u_\delta^2 \sin(\delta + \beta_R) & u < 0 \end{cases} \tag{15}$$

The local rudder blade drift angle β_R is determined as:

$$\beta_R = -\text{atan2}(v_\delta, u_\delta) \tag{16}$$

where u_δ is the effective inflow of the water jet to the rudder blade in the longitudinal direction

$$u_\delta = \begin{cases} \sqrt{k_1 (k_2 u + \sqrt{k_3 u^2 + k_4 T})^2 + k_5 u^2} & T > 0 \\ u & T \leq 0 \end{cases} \tag{17}$$

and v_δ is the effective inflow of the water jet to the rudder blade in the transverse direction, determined from:

$$v_\delta = v - \frac{rL}{2} \tag{18}$$

For a system that includes a propeller and the associated rudder blade, the following force and torque vector is applied to the ship hull

$$\begin{bmatrix} \tau_X \\ \tau_Y \\ \tau_N \end{bmatrix} = \begin{bmatrix} T - D \\ k_{yT} T + k_{yL} L \\ (k_{nT} T + k_{nL} L) L_{xR} \end{bmatrix} \tag{19}$$

Table 3. Parameters of the propeller/rudder control system

No	Variable	Value	No	Variable	Value
1	k_{Tp}	4.5658	8	k_{Fp}	272.1
2	k_{Tn}	3.2903	9	k_{Fn}	204.1
3	k_{yT}	–0.1333	10	k_1	0.3850
4	k_{nT}	–0.2024	11	k_2	0.3000
5	k_{yL}	1.1760	12	k_3	0.4900
6	k_{nL}	–0.5493	13	k_4	0.0217
7	L_{xR}	5.7800	14	k_5	0.1150

4 STRUCTURE OF CONTROL SYSTEM

The above defined control was implemented in the system shown in Figure 3. The input signal to this system is the desired route given by the path planning system as the safe path of ship movement. The desired route has the form of a broken line, defined by the coordinates of subsequent waypoints (x_k, y_k). The ship motion on the water surface is described by the vector $\boldsymbol{x}$ consisting of six state variables (1), where (x, y) are the ship position coordinates measured by the DGPS system, ψ is the ship's heading measured by the gyrocompass, (u, v) are the linear body-fixed velocity components (surge, sway), and r is the yaw rate. Usually, the velocity components are not measured. The measured coordinates of the ship motion state are collected in the vector $\boldsymbol{\eta} = [x, y, \psi]^T$.

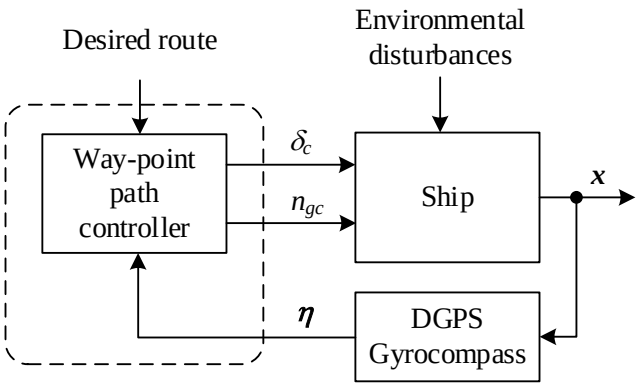

Figure 3. Block diagram of ship's motion control system along desired route

Based on the information received from the path planning system in the form of the desired route and the measured ship position coordinates and course collected in vector $\boldsymbol{\eta} = [x, y, \psi]^T$, the waypoint path controller determines the commanded rudder angles δ_c. The second commanded value, which is the main propeller revolutions n_{gc}, is constant and not regulated. The commanded rudder angle δ_c, is determined using a set of two component controllers, as shown in Figure 4.

Two modes of waypoint path controller operation are considered. The first mode, called track-keeping, consists in controlling the ship's movement along a straight line segment of the route, while the second mode is used during the maneuver of changing to the next straight line route segment and is called the turning maneuver. Conditions for switching between these two operation modes are shown in Figure 5. In Mode 1 (σ = 1), both component controllers are involved in determining the commanded value of rudder blade deflection δ_c. The PD component

controller minimizes the course error e_ψ, while the PI controller minimizes the ship cross-track error e_y. The path controller switches to the turning maneuver when the ship arrives at a distance L_s from a waypoint, which is smaller than the distance L_k for this waypoint ($L_s < L_k$).

The ahead distance L_k at which the turning maneuver should be started depends on the course difference between two consecutive segments of the desired path $L_k = f(\Delta\psi_k)$. This distance was determined experimentally in the here reported tests. After switching to the turning maneuver, the integral in the PI controller is reset to zero using the signal *Reset* and the switching signal σ stops passing the side deviation e_y to the PI controller input ($\sigma = 2$). During the turning maneuver, the specified deflection of the rudder blade δ_c is determined with the assistance of the PD component controller. The turning maneuver is terminated when both the course error e_ψ and its derivative $\dot{e}_\psi$ are smaller than their limits. In the present case, these limits were assumed as: $e_\psi < 5$ and $\dot{e}_\psi < 0.5$.

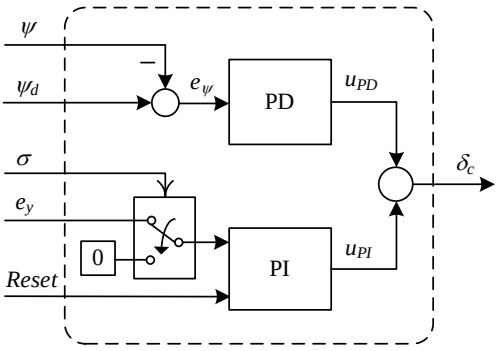

Figure 4. Internal structure of the waypoint path controller

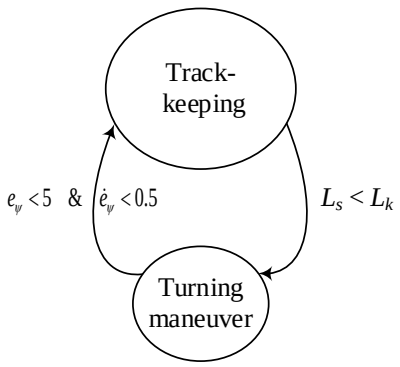

Figure 5. Directed graph illustrating conditions for switching between path controller operation modes.

5 SYNTHESIS OF CONTROL ALGORITHM

The tested path controller is composed of two components connected in parallel. The first component is the PD course controller, used to minimize the course error, while the second is the PI controller, used to minimize the cross-track error from the desired path segment.

For the purpose of path controller synthesis, the dynamics of the tested ship, given by Eq. (7), has been simplified, assuming the constant surge velocity of the ship, $u = u_0 \approx$ constant, and low values of velocities v and r. This allowed linearizing the nonlinear matrix $\boldsymbol{D}$ given by Eq. (9) to the following form

$$\boldsymbol{D} \approx \boldsymbol{D}_L = \begin{bmatrix} -X_u & 0 & 0 \\ 0 & -Y_v & -Y_r \\ 0 & -N_v & -N_r \end{bmatrix} \tag{20}$$

After the linearization of Eq. (7), the longitudinal ship dynamics was decomposed assuming its longitudinal symmetry. The longitudinal force, which depends on the rotational speed of the main propeller screw n_g, was linearized to the form $\tau_X = X_n n_g$. The forces acting on the ship's hull are usually linearly dependent on the rudder deflection δ, according to the relations $\tau_Y = -Y_\delta \delta$ and $\tau_N = -N_\delta \delta$. As a result, the finally obtained maneuvering model consists of the excluded longitudinal ship dynamics

$$(m - X_{\dot{u}})\dot{u} - X_u u - mvr - mx_G r^2 = X_n n_g \tag{21}$$

and the angular-positive dynamics, which is the Davidson and Schiff model (1946) obtained from linearization of Eq. (7)

$$\boldsymbol{M}_1 \dot{\boldsymbol{v}}_1 + \boldsymbol{N}(u_0)\boldsymbol{v}_1 = \boldsymbol{B}\delta \tag{22}$$

where $\boldsymbol{v}_1 = [v, r]^T$ is the state vector, and δ is the rudder deflection. The matrices $\boldsymbol{M}_1$, $\boldsymbol{N}(u_0)$ and $\boldsymbol{B}$ in Eq. (13) are defined as follows (Davidson & Schiff, 1946)

$$\boldsymbol{M}_1 = \begin{bmatrix} m - Y_{\dot{v}} & mx_G - Y_{\dot{r}} \\ mx_G - N_{\dot{v}} & I_z - N_{\dot{r}} \end{bmatrix} \tag{23}$$

$$\boldsymbol{N}(u_0) = \begin{bmatrix} -Y_v & -Y_r + (m - X_{\dot{u}})u_0 \\ -N_v + X_{\dot{u}} u_0 & -N_r + mx_G u_0 \end{bmatrix} \tag{24}$$

$$\boldsymbol{B} = \begin{bmatrix} -Y_\delta \\ -N_\delta \end{bmatrix} \tag{25}$$

Table 4. Parameter values of the simplified mathematical model of *Blue Lady* (u_0 = 1.1 m/s)

No	Variable	Value	No	Variable	Value
1	X_u	–217.0	5	N_r	–68103.0
2	Y_v	–2 972.0	6	Y_δ	–549.7
3	Y_r	9 238.0	7	N_δ	1 487.7
4	N_v	–11 622.0	8	X_n	33.6

The obtained linearized Davidson and Schiff model (1946) of ship dynamics, given by Eq. (22), has a sway velocity v which in the proposed control algorithm (10) was not planned to be stabilized. Therefore, the next step was to eliminate this velocity, after which the Nomoto model was designated (Nomoto et al., 1957)

$$\frac{r(s)}{\delta(s)} = \frac{K(sT_3+1)}{(sT_1+1)(sT_2+1)} \tag{26}$$

where K is the static gain of angular speed, T_1, T_2 and T_3 are time constants, and r is the angular ship velocity $r = \dot{\psi}$. The transmittance parameters (26) refer to hydrodynamic coefficients, according to the following relations

$$T_1 T_2 = \frac{|\boldsymbol{M}_1|}{|\boldsymbol{N}|} \tag{27}$$

$$T_1 + T_2 = \frac{n_{11}m_{22} + n_{22}m_{11} - n_{12}m_{21} - n_{21}m_{12}}{|\boldsymbol{N}|} \tag{28}$$

$$K_R = \frac{n_{21}b_1 - n_{11}b_2}{|\boldsymbol{N}|} \tag{29}$$

$$K_R T_3 = \frac{m_{21}b_1 - m_{11}b_2}{|\boldsymbol{N}|} \tag{30}$$

$$K = -K_R \tag{31}$$

where coefficients m_{ij}, n_{ij} and b_i (i=1,2; j=1,2) are the coefficients of matrices $\boldsymbol{M}_1$, $\boldsymbol{N}$ and $\boldsymbol{B}$ (23)-(25), while $|\boldsymbol{M}_1|$ and $|\boldsymbol{N}|$ are the determinants of matrices $\boldsymbol{M}_1$ and $\boldsymbol{N}$, respectively.

The identification of the Nomoto model parameters based on the sea maneuvering tests has shown that the parameter values T_2 and T_3 in Eq. (26) do not differ much from each other (Fossen, 2011). This allowed further simplification of the transfer function (26), after which the first order Nomoto model was obtained

$$\frac{r(s)}{\delta(s)} = \frac{K}{sT+1} \tag{32}$$

where $T = T_1+T_2-T_3$ is the effective time constant of the angular velocity. The above model can be stored in the time domain as follows

$$\dot{r} = -ar + b\delta \tag{33}$$

where $a = -1/T$, $b = K/T$

To determine the parameters for the PI controller, which minimizes the lateral deviation, it is convenient to record the kinematic equations of ship motion (2) in the following form (Holzhüter, 1990):

$$\dot{x} = u\cos\psi - v\sin\psi \tag{34}$$

$$\dot{y} = u\sin\psi + v\cos\psi \tag{35}$$

$$\dot{\psi} = r \tag{36}$$

The above equations are nonlinear and depend on the values of states u, v and ψ. Nevertheless, linear approximations of these equations can be made, provided that the stationary coordinate system is rotated in such a way that the given course ψ_d becomes equal to zero ($\psi_d = 0$). This way, the ship's control along the desired route will be carried out in the coordinate system (X_R, Y_R) related to the currently executed path segment. Hence, the ship's course ψ^r will have a small value during the control along the desired route, and we can assume that

$$\sin\psi^r \approx \psi^r \qquad \cos\psi^r = 1 \tag{37}$$

Then, assuming that $u \approx U$, the kinematic equations of ship motion can be reduced to a set of linear equations

$$\dot{x}^r = U + d_x \tag{38}$$

$$\dot{y}^r = U\psi^r + v + d_y \tag{39}$$

$$\dot{\psi}^r = r \tag{40}$$

Two additional elements (d_x, d_y) are introduced in the above equations. They describe the errors related to linearization and the slideslip angle caused by environmental disturbances. In Eq. (36), y^r is the ship cross-track error from the desired route, determined from the formula

$$y^r = e_y(t) = [x(t) - x_k]\sin\psi_k - [y(t) - y_k]\cos\psi_k \tag{41}$$

This error depends very strongly on changes in ship's surge speed U.

The task of the path regulator is to control the ship's movement along the current route segment with end coordinates (x_k, y_k) and (x_{k+1}, y_{k+1}), while minimizing the course ψ^r and the cross-track error of ship's position from this segment, $e_y = y^r$. The preset course resulting from a given route segment is determined using Eq. (4), and is changed after reaching a new waypoint. In the path controller, the integral of lateral ship deviation y^r from the path is introduced, through coupling, to its input. Hence, a new state appears in the plant

$$\dot{y}_I^r = y^r \tag{42}$$

The designed waypoint path regulator will not control the surge velocity of the ship, therefore Eq. (38) can be omitted in further analysis. On the basis of Eqs. (40), (33), (39) and (42), we can write the dynamics equations of a simplified mathematical model of the process for the waypoint path controller design

$$\begin{bmatrix} \dot{\psi}^r \\ \dot{r} \\ \dot{y}^r \\ \dot{y}_I^r \end{bmatrix} = \begin{bmatrix} 0 & 1 & 0 & 0 \\ 0 & a & 0 & 0 \\ U & 0 & 0 & 0 \\ 0 & 0 & 1 & 0 \end{bmatrix} \cdot \begin{bmatrix} \psi^r \\ r \\ y^r \\ y_I^r \end{bmatrix} + \begin{bmatrix} 0 \\ b \\ 0 \\ 0 \end{bmatrix} \cdot \delta + \begin{bmatrix} 0 \\ 0 \\ 1 \\ 0 \end{bmatrix} \cdot d_y \tag{43}$$

The controlled variables ψ^r and y^r are determined as follows

$$\begin{bmatrix} \psi^r \\ y^r \end{bmatrix} = \begin{bmatrix} 1 & 0 & 0 & 0 \\ 0 & 0 & 1 & 0 \end{bmatrix} \cdot \begin{bmatrix} \psi^r \\ r \\ y^r \\ y_I^r \end{bmatrix} \tag{44}$$

where $\psi^r = e_\psi = \psi - \psi_k$.

The algorithm designed for the trajectory controller takes the form

$$\delta_z = u_{PD} + u_{PI} = k_1 e_\psi + k_2 r_\psi + k_3 y^r + k_4 y_I^r \tag{45}$$

where

$$e_\psi(t) = \psi_d(t) - \psi(t) \tag{46}$$

$$r_\psi(t) = de_\psi(t)/dt \tag{47}$$

The parameters of the trajectory controller (45), were determined using the pole placement method, based on the linearized process described by Eq. (43) for constant surge velocity $u_0 = 1.1$ (m/s). For further calculations, the following eigenvalues of the designed control system were adopted

$$p_1 = -0.1834,\ p_{1,2} = -0.0692 \pm j0.155,\ p_1 = -0.0047 \tag{48}$$

The desired values of the trajectory controller gains (Table 5) were determined using the function **`place`** included in the Matlab program function set (Mathworks, 2019).

Table 5. Parameters calculated for the PDPI controller.

	k_1	k_2	k_3	k_4
PDPI controller	1.6	19.92	2.125	92.1

6 RESULTS

To check the correctness of the designed control system, both simulation and experimental tests were carried out. The experimental tests were carried out on the training ship *Blue Lady* at the Ship Handling, Research and Training Centre on the Silm lake in Iława/Kamionka. The ship was in full load. During the tests, the wind speed did not exceed 4 m/s. In the experimental tests, the rotational speed of the propeller was constant and equal to $n_g = 440$ rpm.

The first carried out study aimed at experimental determination of the ahead distance L_k for starting the turning maneuver. For this purpose, several maneuvers were made for different course angle changes between two successive straight line segments of the desired route. The obtained test results are shown in Figure 6. The results of the experimental tests, marked as asterisks (*), were approximated using the following formula

$$\begin{aligned} L_k = {} & a_6 \Delta\psi_k^6 + a_5 \Delta\psi_k^5 + a_4 \Delta\psi_k^4 + \\ & + a_3 \Delta\psi_k^3 + a_2 \Delta\psi_k^2 + a_1 \Delta\psi_k + a_0 \end{aligned} \tag{49}$$

The values of parameters $a_0 \ldots a_6$ in Eq. (49) were determined using the function **`polyfit`** included in the Matlab program function set (Mathworks, 2019). These values are collated in Table 6.

Next, the operation of the designed control algorithm along the desired route was tested experimentally. The results of these experiments are given in Figs. 7 and 8. Figure 7 shows the map of the water basin, with the desired route marked by 5 waypoints (x_k, y_k) connected with straight lines (dotted lines in the figure).

This figure also shows the real path (solid line) of the ship sailing along the desired route.

Table 6. Values of parameters describing the approximation of the ahead distance for starting the turning maneuver (49)

No	Variable	Value	No	Variable	Value
1	a_6	5.987527e-09	5	a_2	0.01235089
2	a_5	−1.561371e-06	6	a_1	2.10745127
3	a_4	1.430259e-04	7	a_0	−0.02348713
4	a_3	−0.004935727			

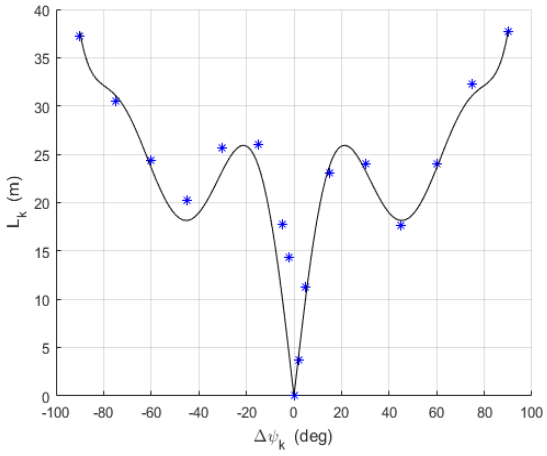

Figure 6. Experimentally determined function $L_k = f(\Delta\psi_k)$ for training ship *Blue Lady*

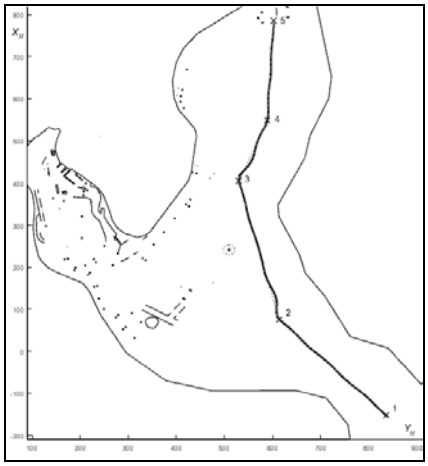

Figure 7. Example of ship path obtained in experimental test performed on the lake Silm in Ilawa/Kamionka

Comparing these two paths reveals large cross-track errors of ship position after the ship passes consecutive waypoints.

The time-history of the cross-track error, shown in Fig. 8, reveals some undamped oscillations.

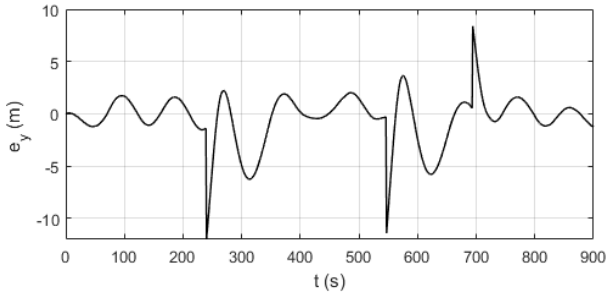

Figure 8. Time-history of cross-track error recorded during the experimental test shown in Figure 7.

7 REMARKS AND CONCLUSIONS

The developed waypoint controller fulfills its task, which consists in steering a ship along the desired route. Unfortunately, there is no good cooperation between the two parts of the designed path controller, as can be observed in the cross-track error time-history revealing relatively large oscillations.

Further work on this path controller design will aim to eliminate oscillations of the cross-track error and to reduce its value. In particular, it will aim at refining the conditions at which the PI part of the algorithm is switched on, as this algorithm component is responsible for minimizing the cross-track error from the desired route segment.

REFERENCES

Ahmed Y.A, & Hasegawa K. 2016. Fuzzy reasoned waypoint controller for automatic ship guidance. *Proceedings of the 10th IFAC Conference on Control Applications in Marine Systems (CAMS*), pp. 604-609. Trondheim, Norway.

Amerongen J.V. & Nauta Lemke H.R.V. 1986. Recent development in automatic steering of ships. *Journal of Navigation*, 39(3): 349-362.

Baker B., Qian C. & Nowak B. 2013. A combined speed and finite-time yaw controller for an underactuated unmanned surface vessel using way-point navigation. *Proceedings of International Conference on Mechatronic and Embedded Systems and Applications (MESA)*. Portland, Oregon, USA.

Bertin D. 1998. Track-keeping controller for a precision manoeuvring autopilot. *Proceedings of the IFAC Conference Control Application in Marine Systems (CAMS)*, pp. 155-160. Fukuoka, Japan,

Chocianowicz W. & Pejaś J. 1982. Adaptive control system for steering the ship along the desired trajectory – based on the optimal control and filtering theory. *Proceedings of Control Applications in Marine Systems (CAMS)*, pp. 319-335. Genova, Italy.

Davidson K.S.M. & Schiff L.I. 1946. Turning and course keeping qualities, *Transactions of Society of Naval Architects Marine Engineers*, 54: 152-190.

Do K.D. & Pan J. 2003. Global waypoint tracking control of underactuated ships under relaxed assumption. *Proceedings of the 42nd IEEE International Conference on Decision and Control (CDC)*, vol. 2, pp. 1244-1249. Maui, Hawaii, USA.

Fossen T.I. 2011. *Handbook of Marine Craft Hydrodynamics and Motion Control*, John Wiley & Sons.

Fredriksen E. & Pettersen K.Y. 2006. Global k-expotential way-point maneuvering of ships: Theory and experiments. *Automatica*, 42(4): 677-687.

Gierusz W. 2001. Simulation model of the shiphandling training boat Blue Lady. *Control Application in Marine Systems 2001,* Katebi R. (Ed.), pp. 255-260. Proceedings of IFAC Conference *on* Control Application in Marine Systems (CAMS). Glasgow, Scotland.

Gierusz W., Nguyen Cong V. & Rak A. 2007. Maneuvering control and trajectory tracking of very large crude carrier, *Ocean Engineering*, 34(7): 932-945.

Holzhüter T. 1990. A high precision track controller for ships, *Proceedings of the 11th IFAC World Congress*, pp. 118-123, Tallin, Estonian USSR.

Kallstrom C.G. 1982. *Identification and adaptive control applied to ship steering*. PhD thesis, Lund Institute of Technology.

Kula K.S. 2015. Model-based controller for ship track-keeping using neural network. *Proceedings of the 2nd IEEE International Conference on Cybernetics (CYBCONF)*, pp. 178-183. Gdynia, Poland.

Kula K.S. & Tomera M. 2017. Control system of training ship keeping the desired path consisting of straight-lines and circular arcs. *TransNav, the International Journal on Marine Navigation and Safety of Sea Transportation*, 11(4): 711-719.

Lazarowska A. 2016. A trajectory base method for ship's safe path planning. *Procedia Computer Science*, 96: 1022 – 1031. Proceedings of the 20th International Conference on Knowledge-Based and Intelligent Information & Engineering Systems - KES2016. York, UK.

Lisowski J. 2016. Analysis of methods of determining the safe ship trajectory. *TransNav, the International Journal on Marine Navigation and Safety of Sea Transportation*, 10(2): 223-228.

MathWorks 2019. *Technical computing software for engineers and scientists*. The MathWorks, Inc., http://www.mathworks.com.

Messer A.C. & Grimble M.J. 1993. Introduction to robust ship track-keeping control design. *Transactions of Instrumental Measurement and Control*, 15(3): 104-110.

Miller A. & Rybczak M. 2015. Methods of controller synthesis using linear matrix inequalities and model predictive control. *Scientific Journals of the Maritime University of Szczecin*, 43(115): 22-28.

Morawski L. & Pomirski J. 1998. Ship track-keeping: experiments with a physical tanker model. *Control Engineering Practice*, 6(6):763-769.

Nomoto K., Taguchi T., Honda K. & Hirano S. 1957. On the steering Qualities of Ships. Technical Report, *International Shipbuilding Progress*, 4(35): 354-370.

Pettersen K. & Lefeber E. 2001. Way-point tracking control of ships. *Proceedings of 40th IEEE Conference on Decision and Control (CDC)*, pp. 940–945. Orlando, Florida, USA.

Śmierzchalski R. & Łebkowski A. 2002. Moving objects in the problem of path planning by evolutionary computation. *Neural Networks and Soft Computing*, Rutkowski L. (Ed.), pp. 382-386. Proceedings of the sixth IEEE International Conference on Neural Networks and Soft Computing. Zakopane, Poland.

Velagic J., Vukic Z. & Omerdic E. 2003. Adaptive fuzzy ship autopilot for track-keeping. *Control Engineering Practice*, 11(4): 433-443.

Vukic Z., Omerdic E. & Kuljaca L. 1998. Improved fuzzy autopilot for track-keeping, *Proceedings of IFAC Conference on Control Application in Marine Systems (CAMS)*, pp. 135-140. Fukuoka, Japan.

Witkowska A. & Śmierzchalski R. 2018. Adaptive backstepping tracking control for an over-actuated DP marine vessel with inertia uncertainties, *International Journal of Applied Mathematics and Computer Science*, 28(4): 679-693.

Yu C. & Xiang X. 2017. Fuzzy-based way-point tracking control of autonomous marine vehicles with input saturation. *Proceedings of the 36th Chinese Control Conference (CCC)*, 4836-4840. Dalian, China.

Zhang Y., Hearn G.E. & Sen P. 1996. A Neural Network Approach to Ship Track-Keeping Control. *IEEE Journal of Ocean Engineering*, 21(4): 513-527.

Zhuo Y. & Guo C. 2013. Underactuated ship way-points track control using repetitive learning neurofuzzy. *Proceedings of the 25th Chinese Control and Decision Conference (CCDC)*, pp. 248-252. Guiyang, China.